Astron. Astrophys. 338, 747–755 (1998)

ASTRONOMY AND ASTROPHYSICS

An eight-moment model parameter study of the solar wind: dependence on variations in coronal heating

Espen Lyngdal Olsen[1], **Egil Leer**[2], **and Øystein Lie-Svendsen**[3]

[1] Harvard-Smithsonian Center for Astrophysics, 60 Garden Street MS 50, Cambridge, MA 02138, USA
[2] Institute of Theoretical Astrophysics, University of Oslo, P.O. Box 1029, Blindern, N-0315 Oslo, Norway
[3] Norwegian Defence Research Establishment (FFI), division for electronics, P.O. Box 25, N-2007 Kjeller, Norway

Received 13 January 1998 / Accepted 21 April 1998

Abstract. The eight-moment two-fluid model describes, self-consistently, the proton (and electron) heat flux in the solar wind. This is a crucial parameter in solar wind models with a high coronal proton temperature. In the present study the eight-moment description is used to study how the solar wind outflow from an electron-proton corona responds to variations in coronal heating. Most of the energy flux is deposited in the proton gas. We find that the asymptotic flow speed of the solar wind is only weakly dependent on the amplitude of the energy flux, but it increases with increasing dissipation length. When most of the energy flux is dissipated in the extended corona, where the protons are collisionless, we obtain flow speeds characteristic of high-speed solar wind streams: For a dissipation length of 1 to 2 solar radii the asymptotic flow speed is 700-1000 km s^{-1}. A relatively modest electron heating in the inner corona may lead to an increased transition region pressure and hence a large increase in the solar wind proton flux. This increase in proton flux may be so large that there is not enough energy available to drive a high-speed wind.

Key words: Sun: corona – solar wind

1. Introduction

We still do not know which mechanism (or mechanisms) provides the energy that is necessary to create the corona and drive the solar wind. Several mechanisms have been proposed, most of which involve conversion of electromagnetic energy into kinetic energy, but no "smoking gun" that may unambiguously settle the issue has been observed. Lacking in situ measurements close to the sun, where most of the heating must take place, we have to settle for the second best, gleaning as much information as possible from remote sensing of the corona and from in situ measurements of the solar wind at large distances from the sun. Only models can provide the link between heating processes in the corona and these observables, and numerical modelling is therefore essential in order to extract whatever information these observations may contain about processes taking place in the corona.

An obvious application of numerical models is to test whether proposed heating mechanisms may account for the observed properties of the corona and solar wind. However, given the large uncertainties about the processes taking place in the transition region and corona, and the physical conditions there, the outcome of such modelling efforts will be far from unique: The available observations are not sufficient to constrain the possible mechanisms completely, and a model will thus only be able to tell whether a mechanism agrees with observations or not, and not whether this is the only solution. Moreover, a single model calculation, based on one specific heating mechanism (e.g., Tu & Marsch 1997 and references therein), cannot tell how sensitive the observed properties are to the details of the proposed mechanism; that is, whether nature has to "get it right," or whether a wide class of processes may lead to the same observed properties.

For these reasons a more fruitful approach may be to start from the opposite end. Instead of hinging our bets on one specific heating mechanism, we may ask: What do the observations tell us about the coronal heating, and what constraints do they impose on *any* viable heating mechanism?

In order to answer this question, model parameter studies are necessary, in which the heating is represented in a rather crude manner (given that the precise mechanism is unknown) where only general properties of the heating process, such as its magnitude and location, are specified, and allowed to vary. The observable properties of the solar wind are then computed as a function of these input parameters.

This is the background and motivation for the present study. Investigating the response of the solar wind to changes in the coronal heating is largely an energy bookkeeping problem. The energy supplied by the heating process may be converted into several different forms of energy, and the properties of the corona and solar wind will depend on how the energy is channelled into these forms. Some of the energy will drive the wind directly, either by lifting the ions out of the sun's gravitational field (or electrons out of the accompanying electrostatic field),

Send offprint requests to: Egil Leer
Correspondence to: Egil Leer, Institute of Theoretical Astrophysics, University of Oslo, P.O. Box 1029, Blindern, N-0315 Oslo, Norway (elols@statoil.no; egil.leer@astro.uio.no; Oystein.Lie-Svendsen@ffi.no)

by increasing the solar wind speed, or by increasing the thermal energy of the ions and electrons (some of which may subsequently be converted into directed motion and add to the solar wind speed). However, some of the supplied energy will also be convected downwards towards the transition region, where it may heat the plasma and thus supply some of the energy needed to drive the wind, or it may be lost through radiation in the lower transition region. Although the fraction of the total energy flux convected downwards may be small compared to the fraction driving the wind directly, this small component may nevertheless have important consequences since it will determine the coronal density and hence the energy per particle in the solar wind.

The heating mechanism may treat the ions (mainly protons) and electrons differently, which adds to the complexity of the energy bookkeeping. Over the last 3-4 years it has been realized that the coronal proton temperature may be significantly higher than the electron temperature in coronal holes, and that the heavy ions are much hotter than the protons (Kohl et al. 1996). The low electron temperature is consistent with a small polarization electric field and a small electron heat flux, so the electrons seem to play a minor role in the force and energy balance in solar wind from large coronal holes. However, through inward heat conduction and collisions in the inner corona, some of the supplied energy will be transferred from the ions to electrons, and, due to their large thermal speed, electrons may efficiently carry this energy into the transition region where it may be decisive in determining the coronal density, as pointed out above. In other words, a model of the solar wind must be able to handle heat conduction in both the proton and electron gas.

How the energy bookkeeping is done in a model may have large implications for the resulting properties of the corona and solar wind. For instance, Hollweg & Johnson (1988) set the proton heat flux equal to zero in the outer corona and find quite high proton temperatures. Hansteen & Leer (1995) use a "classical" proton heat conductive flux in the corona, out to 3-4 R_s. They obtain high proton temperatures, but the asymptotic flow speed of protons is generally lower than the high speeds measured by Ulysses at high solar latitudes (e.g., McComas et al. 1995). In the Hansteen and Leer study the inner boundary is placed in the chromosphere, and it is the low heat flux in the proton gas that gives rise to the high temperatures (see also Hansteen et al. 1997). McKenzie et al. (1995) study a "traditional" solar wind model, where the inner boundary is placed in the lower corona. They assume that the proton heat flux is zero everywhere. By specifying the solar wind proton flux and adding energy to the protons in the inner corona, in the form of heat, they can drive a high-speed wind. As there is no energy loss into the inner boundary the solar wind is the only energy loss, and heating of the protons results in a high proton temperature and a large asymptotic flow speed. The maximum coronal proton temperature, consistent with an asymptotic flow speed of 800 km s^{-1}, is close to 10 million degrees. (Models with no proton heat conduction, and high proton temperatures, have also been studied by e.g., Isenberg (1990), Esser & Habbal (1996), and Esser et al. (1997).)

A comparison of the two-fluid models studied by Hansteen & Leer (1995) and by McKenzie et al. (1995) indicates that the treatment of the proton heat conduction may be critical for the results obtained in model studies of the solar wind. This led Evje & Leer (1998) to consider a solar wind model with a "classical" electron heat flux and a classical proton heat flux in the very inner corona that reduces to zero (over a given length scale) in the collisionless region. The results show that when the protons are heated in the outer corona, where the proton heat flux is small and the coupling to the electrons is weak, most of the energy flux is lost in the solar wind, and large asymptotic flow speeds are obtained. On the other hand, heating close to the sun leads to a high electron density in the inner corona, a large solar wind proton flux, and a relatively small asymptotic flow speed (see Hammer 1982; Withbroe 1988). The proton heat flux used by Evje and Leer allows for an investigation of how sensitive the solar wind model results are to variations of the proton heat flux, but it does not consistently describe the heat flux in the proton gas.

For a parameter study of the coronal heating to be worthwhile, the above studies show that not only the energy balance at the lower boundary must be handled properly. Equally important, the model must be able to treat the proton heat conduction self-consistently, from the collision-dominated, lower corona where classical heat conduction (proportional to ∇T) is probably valid and well into the collisionless, supersonic flow regime. If this is not done consistently, and we make, say, an almost arbitrary separation between classical proton heat conduction at low altitudes and no heat conduction at high altitudes, as in some of the studies above, the resulting corona and solar wind may as much depend on this ad hoc treatment of heat transport as on the heating process itself. In particular, if the location of the coronal heating is varied, it may be difficult to attribute a change in solar wind properties to this change in location, and not to the different treatment of heat transport at the different locations.

The eight-moment fluid approximation is the simplest model that describes heat transport in a self-consistent manner. From the considerations above, the simplest possible solar wind model that can be used for a parameter study of the coronal heating will therefore be based on the eight-moment approximation, which is also chosen in this study. In an eight-moment, two-fluid model the equations for the heat flux density in the electrons and protons are solved together with the mass, momentum, and energy equations, thus placing the heat flux density on an equal footing with the mass, momentum, and energy densities (Olsen & Leer 1996). In the strongly collision-dominated regime the proton heat flux is determined by the temperature gradient and by collisions with electrons, and when collisions cease to be important the heat flux is determined by the acceleration and expansion of the flow (see Schunk 1977). Olsen & Leer (1996) found that the classical Spitzer-Härm expression for the proton heat flux is not valid in the fast solar wind, and that the reduced proton heat flux in the eight-moment model may lead to a higher coronal proton temperature and a more rapid acceleration of the solar wind.

2. Description of the model

We make use of the eight-moment, two-fluid description of the solar wind outflow from the very inner corona. The "mechanical" energy flux from the sun, deposited in the corona as heat, creates the hot corona and drives the solar wind. Instead of solving for the transition region, corona, and the solar wind, we place the inner boundary in the upper transition region, at a temperature of 5×10^5 K (where the electrons and ions are thermally coupled), and adjust the density at this boundary such that the inward heat flux balances the radiative loss from the lower transition region and the increase of the solar wind enthalpy flux through the transition region, up to the inner boundary (e.g., Endler et al. 1979). Since observations show that ion temperatures are considerably higher than the electron temperature in the corona, most of the energy flux is probably deposited in the protons. In the model we therefore deposit most of the mechanical energy flux in the protons, but we also allow for some electron heating. We study variations in the solar wind due to both variations in the amplitude of the mechanical energy flux and the location of the heating (through a dissipation length). In addition, the fraction of the energy flux that is deposited in the electron gas will be varied. We shall consider both spherically symmetric and rapidly expanding flow.

We describe the electron-proton outflow using the set of eight-moment approximation transport equations given by Schunk (1977).

Conservation of mass:

$$\frac{\partial n}{\partial t} + \frac{1}{A}\frac{\partial}{\partial r}(Anu) = 0. \tag{1}$$

Conservation of momentum:

$$\frac{\partial u}{\partial t} + u\frac{\partial u}{\partial r} + \frac{1}{mn}\frac{\partial}{\partial r}(p_e + p_p) + \frac{GM_s}{r^2} = 0. \tag{2}$$

Energy balance in the electrons:

$$\frac{3}{2}\frac{\partial p_e}{\partial t} + \frac{3}{2}u\frac{\partial p_e}{\partial r} + \frac{5}{2}p_e\frac{1}{A}\frac{\partial}{\partial r}(Au) + \frac{1}{A}\frac{\partial}{\partial r}(Aq_e) = -\frac{m_e}{m_e + m_p}n\nu_{ep}3k(T_e - T_p) + Q_{me}. \tag{3}$$

Energy balance in the protons:

$$\frac{3}{2}\frac{\partial p_p}{\partial t} + \frac{3}{2}u\frac{\partial p_p}{\partial r} + \frac{5}{2}p_p\frac{1}{A}\frac{\partial}{\partial r}(Au) + \frac{1}{A}\frac{\partial}{\partial r}(Aq_p) = -\frac{m_p}{m_e + m_p}n\nu_{pe}3k(T_p - T_e) + Q_{mp}. \tag{4}$$

Electron heat flux:

$$\frac{\partial q_e}{\partial t} + u\frac{\partial q_e}{\partial r} + \frac{9}{5}q_e\frac{\partial u}{\partial r} + \frac{7}{5}q_e\frac{1}{A}\frac{\partial}{\partial r}(Au) + \frac{5}{2}\frac{kp_e}{m_e}\frac{\partial T_e}{\partial r} = -\nu_{ep}\left(D_{ep}^{(1)}q_e - D_{ep}^{(4)}\frac{m_e}{m_p}q_p\right) - \frac{4}{5}\nu_{ee}q_e - \frac{5}{2}\frac{p_e}{nm_e}F_{ep}\,. \tag{5}$$

Proton heat flux:

$$\frac{\partial q_p}{\partial t} + u\frac{\partial q_p}{\partial r} + \frac{9}{5}q_p\frac{\partial u}{\partial r} + \frac{7}{5}q_p\frac{1}{A}\frac{\partial}{\partial r}(Au) + \frac{5}{2}\frac{kp_p}{m_p}\frac{\partial T_p}{\partial r} = -\nu_{pe}\left(D_{pe}^{(1)}q_p - D_{pe}^{(4)}\frac{m_p}{m_e}q_e\right) - \frac{4}{5}\nu_{pp}q_p - \frac{5}{2}\frac{p_p}{nm_p}F_{pe}\,. \tag{6}$$

Here, t is the time; r is the heliocentric distance; n is the electron (proton) density; u is the radial flow speed; A is the cross-section of a small radial flow tube; $m = m_e + m_p$ is the mass; p is the pressure; T is the temperature; and q is the heat flux density. The indices e and p refer to the electrons and protons, respectively. The Boltzmann constant is denoted k, G is the gravitational constant, and M_s is the mass of the sun. Q_{me} and Q_{mp} are heating terms in the electron and proton fluids, due to the mechanical energy flux. These are the main parameters that will be varied in the study. Forces acting on the gas due to the mechanical energy flux are neglected.

The electron-electron collision frequency, ν_{ee}, and the proton-proton collision frequency, ν_{pp}, measured in s^{-1}, are given by

$$\nu_{ee} \approx 5.85 \times 10^{-5} n T_e^{-3/2} \tag{7}$$

$$\nu_{pp} \approx 1.38 \times 10^{-6} n T_p^{-3/2}, \tag{8}$$

where the density is measured in m^{-3} and temperature in K. The electron-proton collision frequency is given by

$$\nu_{ep} \approx 8.28 \times 10^{-5} n T_e^{-3/2} \tag{9}$$

and

$$\nu_{pe} = \frac{m_e}{m_p}\nu_{ep}. \tag{10}$$

Finally, $D_{ep}^{(1)} = -\frac{1}{5}$, $D_{ep}^{(4)} = \frac{6}{5}$, $D_{pe}^{(1)} = 3$, and $D_{pe}^{(4)} = -\frac{3}{2}\frac{m_e}{m_p}$.

The thermal force given by Schunk (1997) is

$$F_{ep} = -F_{pe} = \frac{3}{5}\nu_{ep}\frac{m_e}{kT_e}\left(q_e - \frac{m_e}{m_p}q_p\right) \approx \frac{3}{5}\nu_{ep}\frac{m_e}{kT_e}q_e\,.$$

When this force is introduced in Eq. (5) the heat flux (in a static electron gas) is reduced by a factor 3. The reduction of the electron heat flux by a factor three, due to the interaction with protons, was also found by Chapman (1954). Studies by Spitzer & Härm (1953), Braginskii (1965), and others indicate that the effect of the protons on the electron heat flux is much smaller. In the present study we therefore use a thermal force.

$$F_{ep} = \frac{3}{5}\alpha\nu_{ep}\frac{m_e}{kT_e}q_e\,,$$

where $\alpha = 0.15$. This leads to a reduction of the electron heat flux of about 10% relative to the case with no electron-proton collisions.

The heating rates Q_{me} and Q_{mp} in Eqs. (3) and (4) can be written as the divergence of the mechanical energy flux densities,

$$Q_{me} = -\nabla \cdot \boldsymbol{f}_{me} \tag{11}$$

and

$$Q_{mp} = -\nabla \cdot \boldsymbol{f}_{mp}, \tag{12}$$

where $\boldsymbol{f}_{me} = f_{me}(r)\boldsymbol{e}_r$, $\boldsymbol{f}_{mp} = f_{mp}(r)\boldsymbol{e}_r$, and where $\boldsymbol{e}_r$ is the unit vector in the radial direction. We make the assumption that the energy fluxes are dissipated over length

scales H_{me} and H_{mp}, starting from the inner boundary $r_0 = 1\ R_s$ (e.g., Hammer 1982; Withbroe 1988; Wang 1993; Sandbæk et al. 1994),

$$Af_{me}(r) = A_0 f_{me0} \exp[-(r - r_0)/H_{me}] \quad (13)$$

$$Af_{mp}(r) = A_0 f_{mp0} \exp[-(r - r_0)/H_{mp}], \quad (14)$$

where f_{me0} and f_{mp0} are the mechanical energy flux densities at the inner boundary and A_0 is the area of the flow tube at $r = r_0$. The electron (proton) heating is then given as $Q_{me(p)} = f_{me(p)}/H_{me(p)}$. By varying the damping lengths we can vary the energy per particle deposited in the corona and thus create very different temperature structures.

Starting from an initial guess for the solution, we integrate Eqs. (1)-(6) forward in time until a steady state is reached. A description of the numerical method used to solve these equations is given in Olsen & Leer (1996).

3. Results

We solve the coupled set of Eqs. (1)-(6) together with the auxiliary Eqs. (7)-(14) for a number of cases where we vary the values of the free parameters over a wide range. The free parameters in our model are the magnitude of the energy flux density from the sun, $f_{m0} \equiv f_{me0} + f_{mp0}$, given at the inner boundary, the fraction of the energy flux that is deposited in the electron fluid (or in the proton fluid), f_{me0}/f_{m0} (or f_{mp0}/f_{m0}), and the damping lengths, H_{me} and H_{mp}, for these energy fluxes.

As pointed out previously, the pressure at the inner boundary is obtained by assuming that the radiative losses in the chromosphere-corona transition region and the increase of the solar wind enthalpy flux, inside the inner boundary, are balanced by the (electron) heat conductive flux from the hot corona (e.g., Evje & Leer 1998),

$$\frac{p_0}{C} + 5 n_0 u_0 k T_0 \approx -q_{e0} \quad (15)$$

where $p_0 = 2 n_0 k T_0$ is the gas pressure in the transition region, u_0 is the drift speed at the inner boundary, $C \approx 7 \times 10^{-5}$ s m^{-1}, and q_{e0} is the electron heat flux density at the inner boundary (positive outwards). In this way we account for the energy balance in the transition region without solving for the detailed structure of the region. We assume that the coronal gas expands into a vacuum so the flow speed at the outer boundary is supersonic.

Our main goal is to study how the solar wind proton flux and asymptotic flow speed vary with the amplitude and dissipation length of the energy fluxes deposited in the corona, and to see whether rapidly expanding flow is different from a spherically symmetric solar wind.

3.1. Spherically symmetric flow; $A \propto r^2$

Let us start with spherically symmetric flow and take the same dissipation length for the electron and proton energy flux, $H_{me} = H_{mp} = H_m$. We find how the solar wind proton flux and asymptotic flow speed, as well as the electron density, n_0, and heat conductive flux density, q_{e0}, at the inner boundary, change when we vary the energy flux, f_{m0}, and the damping length, H_m. We consider a range of H_m and f_{m0} values that produce solar wind solutions with proton fluxes and asymptotic flow speeds that are comparable to the observed values: We allow H_m to vary between 0.5 R_s and 2.0 R_s, and f_{m0} to vary between 50 W m^{-2} and 200 W m^{-2}. With this parameter range we cover asymptotic flow speeds (of the quasi-steady solar wind) in the range 300-1000 km s^{-1} and proton flux densities at the orbit of Earth from 2 to 8×10^{12} m^{-2} s^{-1} in the low-speed wind, and from 1 to 4×10^{12} m^{-2} s^{-1} in the high-speed wind.

Figs. 1 and 2 show the results for $f_{me0}/f_{m0} = 0$ and 0.2, respectively. In each of these cases we show contour plots of the solar wind proton flux density at the orbit of Earth, $(nu)_E$ (a-panels), the flow speed at the orbit of Earth, u_E (b-panels), the electron density at the inner boundary, n_0 (c-panels), and the electron heat flux density (from the corona) at the inner boundary, q_{e0} (d-panels).

Figs. 1-2 show that there are rather small differences between the case where all the energy flux is deposited in the proton gas (Fig. 1) and the case where 20% is deposited in the electrons (Fig. 2). The d-panels show that in the case with electron heating a larger fraction of the energy flux is conducted back into the inner boundary, and the solar wind energy flux is therefore reduced. This enhanced inward heat flux is consistent with a somewhat higher electron density at the inner boundary (cf. panels c), due to the boundary condition (15).

The a-panels show that the solar wind proton flux is slightly higher in the case with electron heating. Hence the energy per unit mass and the asymptotic flow speed are reduced when part of the energy flux from the sun is deposited in the electron gas (cf. panels b).

For the models presented in Figs. 1-2 the solar wind proton flux is, to a good approximation, proportional to the energy flux from the sun, and it decreases with increasing damping length, roughly as $H_m^{-0.7}$. When some of the energy flux is deposited in the electron gas there is a small increase in the proton flux (at the expense of flow speed), but for the parameter range considered here ($f_{me0}/f_{m0} \leq 0.2$) the increase is less than 10%. As the solar wind proton flux, $(nu)_E$, is almost proportional to the energy flux, f_{m0}, and most of the energy flux deposited in the corona goes into driving the solar wind, the asymptotic flow speed is almost independent of the amplitude of the energy flux. This is partly a consequence of the boundary condition (15): As the energy flux is increased, the increased downward energy flux, although small, causes an increase in the electron density at the inner boundary, such that the solar wind proton flux is proportional to the mechanical energy flux. For a different boundary condition, say a fixed electron density, n_0, the proton flux would increase less rapidly and the energy per unit mass in the flow would increase with increasing energy flux. The decrease of the proton flux with increasing dissipation length, H_m, is consistent with an increase of the asymptotic flow speed. This is seen in the b-panels in Figs. 1-2.

The fraction of the energy flux that is lost as inward heat conductive flux is relatively small, but this inward heat flux

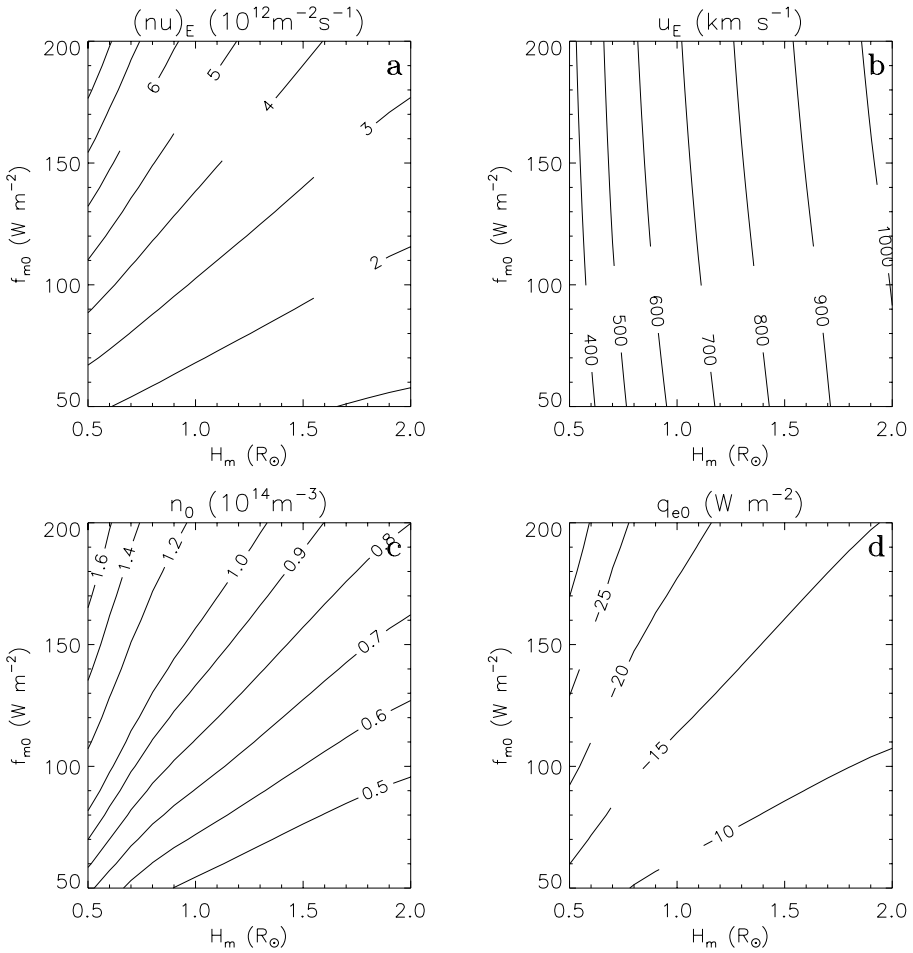

Fig. 1a–d. Contour plots showing solar wind parameters as a function of H_m and f_{m0} for $f_{me0}/f_{m0} = 0$ and spherically symmetric outflow: **a** The proton flux, $(nu)_E$, at 1 AU; **b** the flow speed, u_E, at 1 AU; **c** the electron density, n_0, at the inner boundary; and **d** the electron heat flux, q_{e0}, at the inner boundary. (The inner boundary is in the upper part of the transition region, at the $T_0 = 5 \times 10^5$ K level.)

is very important for maintaining the transition region pressure (and hence the electron density at the inner boundary) consistent with the mass and energy flux in the solar wind. The d-panels in Figs. 1-2 show that the inward heat flux increases with increasing energy flux from the sun, it decreases with increasing dissipation length, and it increases when part of the energy flux from the sun is deposited directly in the electron fluid. The fraction of the mechanical energy flux that is lost as inward heat conductive flux is between 33% (for $f_{m0} = 50$ W m^{-2}, $H_m = 0.5\ R_s$, and $f_{me0}/f_{m0} = 0.20$), and 7% (for $f_{m0} = 200$ W m^{-2}, $H_m = 2.0\ R_s$, and $f_{me0}/f_{m0} = 0$). In the spherically symmetric solar wind considered here, most of the inward heat flux is lost as radiation from the lower part of the transition region; the solar wind enthalpy flux at the inner boundary is small by comparison. Thus, the density at the inner boundary, n_0, is, to a good approximation, proportional to the heat conductive flux density from the corona. This is also seen in Figs. 1-2 (panels c and d). The electron density at the inner boundary varies from 0.4×10^{14} m^{-3} to 2×10^{14} m^{-3}. For the parameter values that produce solar wind with proton fluxes and asymptotic flow speeds that are typical of quasi-steady high-speed streams, $(nu)_E \approx 2 \times 10^{12}$ m^{-2}s^{-1} and $u_E \approx 750$ km s^{-1}, we find an electron density at the inner boundary of $n_0 \approx 0.6 \times 10^{14}$ m^{-3}. This corresponds to a rather low electron density in the inner corona.

We have chosen not to include plots of the solar wind enthalpy flux (or electron and proton temperature) and the heat conductive flux at $r = 1$ AU. The solar wind is highly supersonic at the orbit of Earth so the enthalpy flux is much smaller than the kinetic energy flux. The solar wind electron and proton heat conductive fluxes are also small at the orbit of Earth (Olsen & Leer 1996). The modelled temperatures in the outer solar wind depend on the dissipation length, H_m, and on the fraction of the energy flux that is deposited in the protons and the electrons.

3.2. Rapidly expanding flow

Let us now consider a rapidly expanding outflow where the cross-section, A, of a radial flow tube increases as (Kopp & Holzer 1976)

$$A = A_0 \left(\frac{r}{r_0}\right)^2 \frac{f_{\max} \mathrm{e}^{(r-r_1)/\sigma} + f_1}{\mathrm{e}^{(r-r_1)/\sigma} + 1} \tag{16}$$

where $f_1 = 1 - (f_{\max} - 1)\mathrm{e}^{(r_0-r_1)/\sigma}$. We use the parameter values $f_{\max} = 5$, $r_1 = 1.31\ R_s$, and $\sigma = 0.51\ R_s$ that were derived by Munro & Jackson (1977) for a large coronal hole.

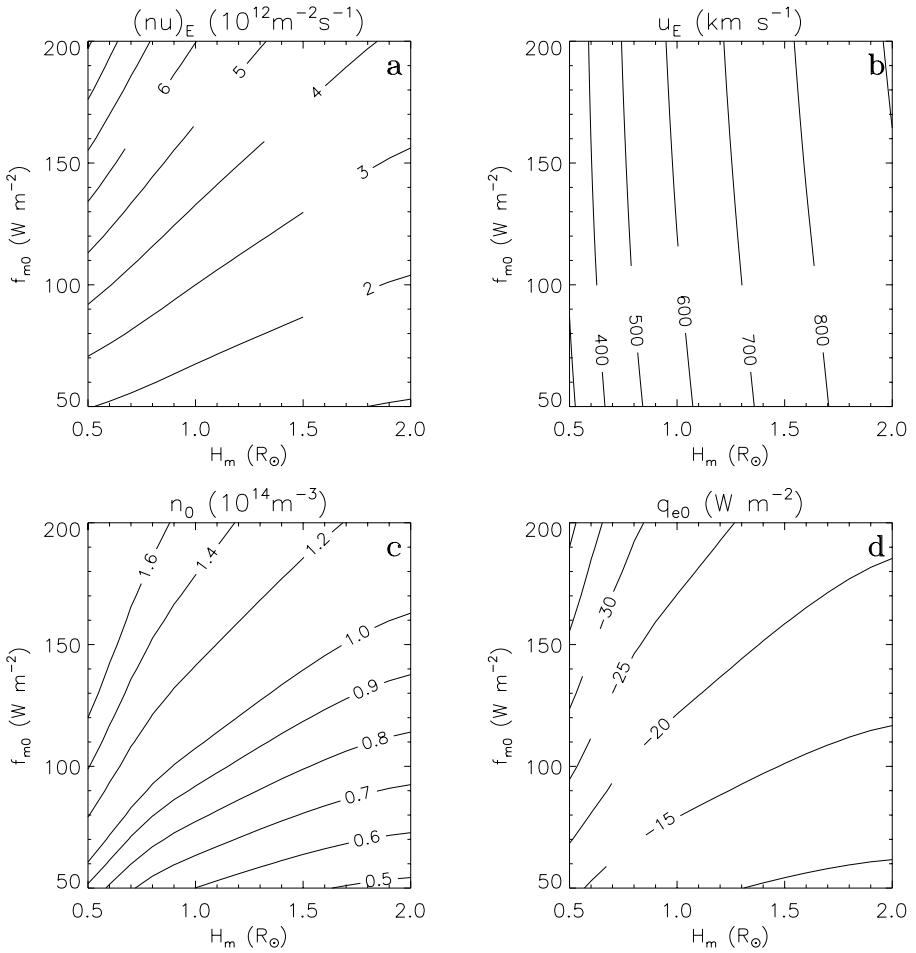

Fig. 2a–d. Same as Fig. 1, but $f_{me0}/f_{m0} = 0.2$.

We let 20% of the mechanical energy flux heat the electrons and take $H_{me} = H_{mp} = H_m$. In order to obtain reasonable solar wind parameters we consider the range of $f_{m0}/f_{\max}$ values from 50 to 200 W m^{-2} and H_m values from 0.5 to 2.0 R_s (cf. Figs. 1-2). Apart from the different geometry, these parameters are identical to those used in Fig. 2. The results are shown in Fig. 3.

The effect of increasing the expansion rate of the flow tube can be seen by comparing Figs. 2 and 3. For a fixed $f_{m0}/f_{\max}$ value and a fixed damping length, H_m, a smaller fraction of the energy flux is lost as inward heat flux in rapidly expanding flow than in spherically symmetric flow. In the rapidly expanding case we find that between 4% and 10% of the supplied energy flux is lost through inward heat conduction. Hence more than 90% of the energy flux deposited in the corona is lost in the solar wind. Fig. 3 (panel d) shows that for a fixed energy flux, f_{m0}, an increasing fraction is lost as inward heat conductive flux when the damping length H_m decreases, and for a fixed value of H_m the fraction of the energy flux that is lost as inward heat flux decreases with increasing values of f_{m0}. But the heat conductive flux at the inner boundary does not exceed 10% of the mechanical energy flux. In the spherically symmetric case we found that more than 30% of the energy flux may be lost as inward heat flux. In models of rapidly expanding, high-speed flow the heat conductive flux into the transition region is smaller than the value derived from observations (e.g., Withbroe 1988).

Qualitatively, the results for rapidly expanding flow are very similar to the results obtained for spherically symmetric flow: The solar wind proton flux increases with the energy flux, $f_{m0}/f_{\max}$, and it decreases with increasing damping length, H_m, but the increase and decrease are more gradual in the rapidly expanding flow than in the flow where $A \propto r^2$. Consequently, for a fixed damping length the asymptotic flow speed now increases with increasing energy flux, while it was nearly independent of f_{m0} for $A \propto r^2$. For a specified value of $f_{m0}/f_{\max}$ and H_m we generally find a larger asymptotic flow speed in the rapidly expanding flow.

In the spherically symmetric solar wind most of the inward heat flux is lost as radiation, and the electron density at the inner boundary is proportional to the inward heat flux (cf. panels c and d in Figs. 1 and 2). However, in the rapidly expanding flow most of the inward heat conductive flux goes into heating the solar wind in the transition region (by balancing the enthalpy flux in (15)). Hence the inward heat flux is proportional to the solar wind proton flux. Fig. 3 (panels a and d) show the strong correlation between $(nu)_E$ and q_{e0}. The electron density, n_0, at the inner boundary is "floating" in the rapidly expanding flow; it assumes the value that is consistent with a conserved proton flux. This electron density is smaller than the density (at the

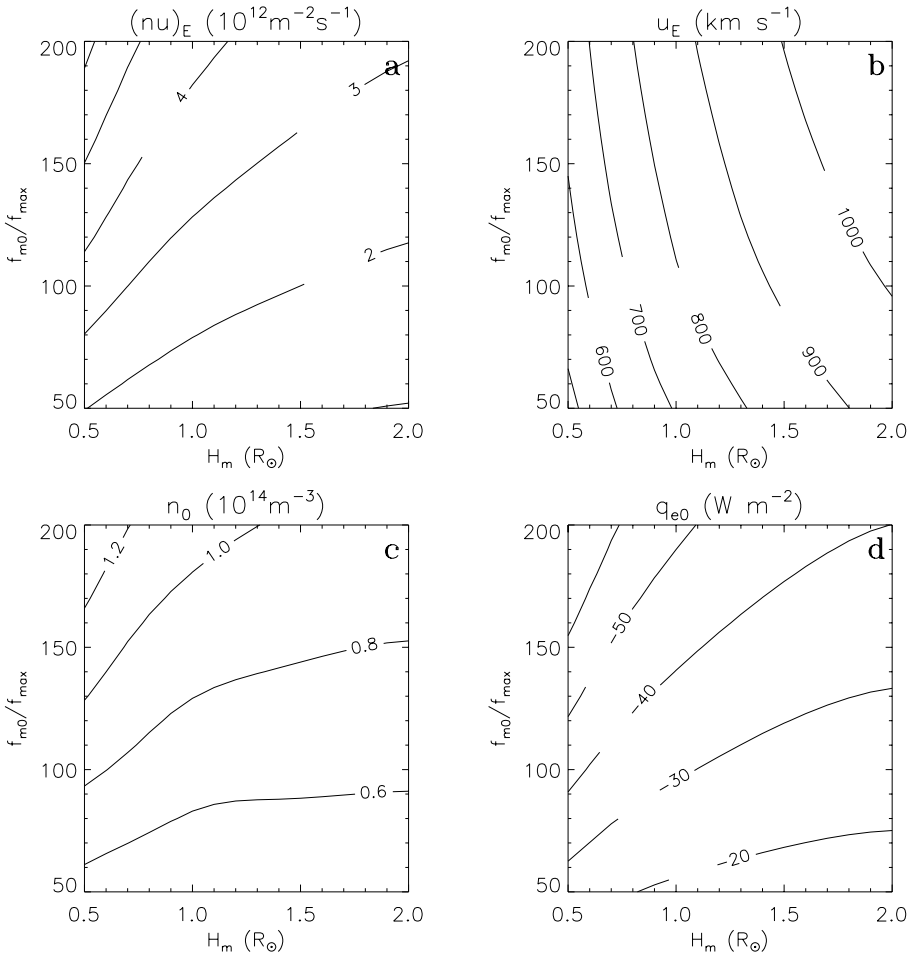

Fig. 3a–d. Same as Fig. 2, but for rapidly expanding flow ($f_{\max} = 5$).

inner boundary) in spherically symmetric flow, for the same values of $f_{m0}/f_{\max}$ and H_m (see panels c in Figs. 2 and 3).

In the spherically symmetric case we found solar wind parameters (proton flux and asymptotic flow speed) characteristic of quasi-steady, high-speed solar wind streams for, say, $f_{m0} \approx 80$ W m^{-2} and $H_m \approx 1.5\ R_s$. In the rapidly expanding flow we must also have $f_{m0}/f_{\max} \approx 80$ W m^{-2} to drive typical quasi-steady, high-speed streams, but the critical point is closer to the sun in this case, so the high asymptotic flow speed can be obtained for a smaller damping length; $H_m \approx 1\ R_s$ for $f_{\max} = 5$. In both these cases a significant fraction of the energy flux from the sun is deposited in the supersonic region of the flow, where the protons are collisionless. The proton heat flux from the supersonic region and into the subsonic region, as well as the transfer of heat to the electrons, are small. The relatively small heat flux through the inner boundary is consistent with a low electron density in the inner corona, a small solar wind proton flux, and a large energy per mass in the solar wind. Heating of the electron gas leads to an increase of the inward heat flux and of the solar wind proton flux and therefore to a decrease of the asymptotic flow speed. But it is the dissipation length that is the crucial parameter for determining whether or not we can drive a high-speed flow: In both the spherically symmetric and rapidly expanding flow most of the mechanical energy flux must be deposited in the proton gas in the outer corona in order to obtain the large proton temperatures that are necessary to drive high-speed streams.

These studies illustrate that heating of the proton gas in the outer corona can drive a high-speed solar wind. Electron heating leads to a larger inward heat flux, a higher electron density at the inner boundary, a larger solar wind proton flux, and a smaller asymptotic flow speed. When most of the energy flux is deposited in the electron gas it is very difficult to drive a high-speed wind (c.f. Sandbæk & Leer 1995).

3.3. Different values for H_{mp} and H_{me}

We have shown that a mechanical energy flux of, say, $f_{m0}/f_{\max} = 80$ W m^{-2} deposited over $H_m \geq 1\ R_s$ in a rapidly expanding flow can drive a high-speed solar wind with a reasonable proton flux. Let us study the case presented in Fig. 3, but we now fix the energy flux from the sun, $f_{m0}/f_{\max} = 80$ W m^{-2}, as well as the fraction of the flux that is heating the protons and electrons, $f_{mp0}/f_{m0} = 0.8$, and instead allow for different damping lengths H_{me} and H_{mp}.

When varying the damping lengths H_{me} and H_{mp} independently we allow for a somewhat larger range than in Figs. 1-3. Fig. 4 shows how the proton flux, $(nu)_E$, and flow speed,

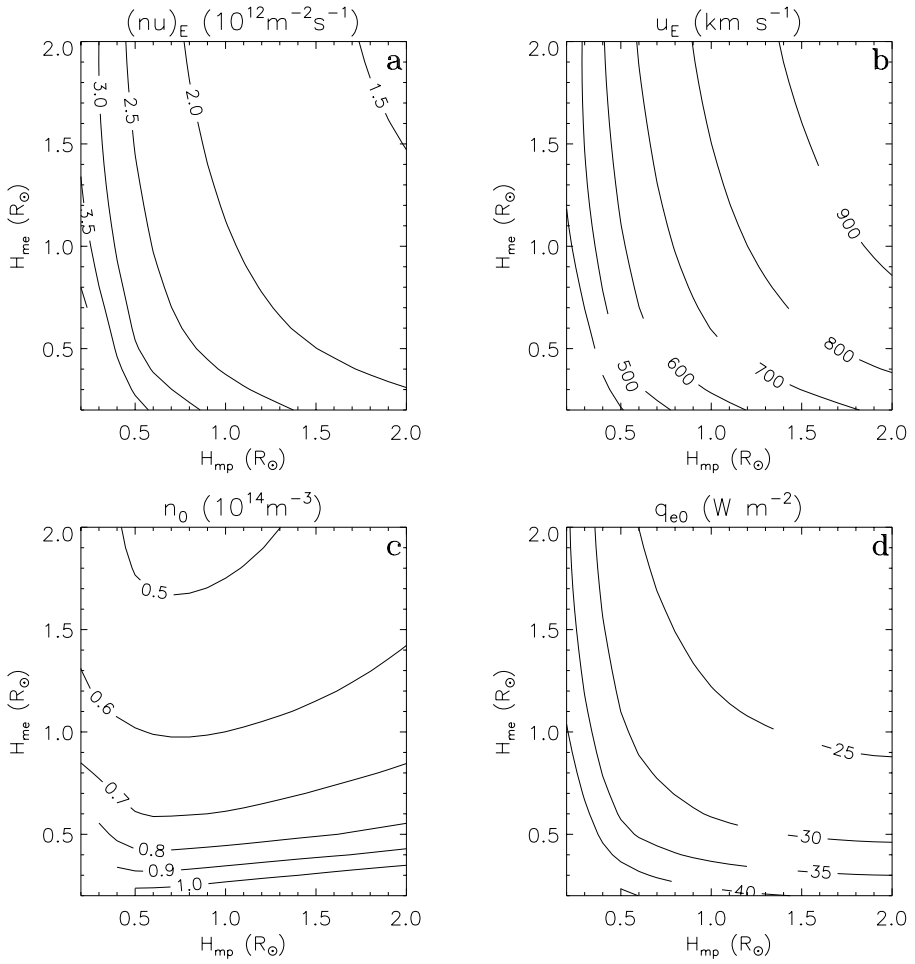

Fig. 4a–d. Contour plots showing solar wind parameters as a function of H_{me} and H_{mp} for $f_{m0}/f_{\max} = 80$ Wm^{-2}, $f_{me0}/f_{m0} = 0.2$, and rapidly expanding flow ($f_{\max} = 5$). The panels are arranged as in Figs. 1-3: **a** The proton flux, $(nu)_E$, at 1 AU; **b** the flow speed, u_E, at 1 AU; **c** the electron density, n_0, at the inner boundary; and **d** the electron heat flux, q_{e0}, at the inner boundary.

u_E, at the orbit of Earth, as well as the electron density, n_0, and heat flux density, q_{e0}, at the inner boundary, vary with the damping lengths, in the range $0.2\ R_s \leq H_{me} \leq 2.0\ R_s$ and $0.2\ R_s \leq H_{mp} \leq 2.0\ R_s$. (The variations seen in Fig. 4 for $H_{me} = H_{mp} = H_m$, when H_m is varied, are the same as the variations seen in Fig. 3 for $f_{m0}/f_{\max} = 80$ W m^{-2}.) For small damping lengths it is time consuming to obtain steady-state solutions of the set of time-dependent equations. In these cases the asymptotic flow speed of the solar wind is low. We have not made an effort to obtain solutions for cases where the asymptotic flow speed is below some 350 km s^{-1}.

Fig. 4, panels a and b, show that the solar wind proton flux decreases and the asymptotic flow speed increases with increasing damping lengths, H_{me} and H_{mp}. As 80% of the energy flux is deposited in the proton gas the results are most sensitive to variations in H_{mp}: For a fixed value of H_{me} the proton flux decreases by more than a factor 2 and the flow speed increases by a factor 2 when H_{mp} increases from $0.2\ R_s$ to $2\ R_s$. For a fixed value of H_{mp} the variations of $(nu)_E$ and u_E due to variations of H_{me} are smaller than a factor 2. If the 20% of the energy flux deposited in the electron gas is deposited very close to the sun, the solar wind proton flux increases so much that a very large proton damping length, $H_{mp} \simeq 2\ R_s$, is needed to bring the asymptotic wind speed u_E above 700 km s^{-1}. Increasing H_{me} leads to a significant decrease of the proton flux and an increase of the asymptotic flow speed, but for somewhat larger values of H_{me} (e.g., $H_{me} \geq 1\ R_s$) the results are not so dependent on variations in the electron damping length as they are for smaller H_{me}.

As we have mentioned before, the inward heat conductive flux at the inner boundary in a rapidly expanding flow is a small fraction of the mechanical energy flux, and most of this energy flux goes into heating the solar wind plasma inside the inner boundary. As in Fig. 3 this is evidenced by the strong correlation between q_{e0} and $(nu)_E$.

4. Summary

In the parameter study presented here we specify the spatial profile of the mechanical energy flux from the sun (constant damping length(s)), and find that in spherically symmetric outflow the solar wind proton flux is, to a good approximation, proportional to the amplitude of the energy flux, f_{m0}. An increase in damping length (for fixed f_{m0}) leads to a larger fraction of the energy flux being dissipated in the supersonic region of the flow, so the solar wind proton flux decreases and the energy per unit mass in the flow increases, and therefore the asymptotic flow speed increases (see Leer & Holzer 1980). For a mechanical en-

ergy flux density of, say $80\ \mathrm{W\ m^{-2}}$, in a spherically symmetric corona-solar wind model, dissipated over $H_m \geq 1.5\ R_s$ or so with most of the energy flux going into the proton gas, we obtain a solar wind proton flux and asymptotic flow speed in quite good agreement with in situ observations made in quasi-steady high-speed solar wind streams. In these models the inward heat conductive flux from the corona is quite small, and most of it is lost as radiation from the transition region. Thus, the electron density in the inner corona is proportional to the heat conductive flux density.

In rapidly expanding flow geometries the "critical point" is closer to the sun than in spherically symmetric outflow (for the same coronal temperature structure). Thus, for comparable mechanical energy fluxes and a given damping length, more of the energy flux may be deposited in the supersonic region. A smaller fraction of the energy flux is "lost" through the inner boundary. In rapidly expanding flow most of the inward heat flux goes into heating the solar wind in the transition region. Hence the inward heat flux is proportional to the solar wind proton flux.

The eight-moment, two-fluid model provides a self-consistent description of the electron-proton solar wind. In the cases considered here most of the energy is supplied to the protons, and the electron temperature in the corona is quite low. The electrons can be described as a collision-dominated gas (Lie-Svendsen et al. 1997). With the reduction of the thermal force to 15% of the value given by Schunk (1997), the heat flux in the electron gas is close to its "classical" value. If the full thermal force had been used, the electron heat flux into the transition region would be reduced. This would lead to a reduced transition region pressure and coronal electron density. The rsult obtained would then be quite different from the present study.

The proton heat flux is only a small fraction of its classical value, even near the lower boundary of the model. The inability of the protons to conduct heat away leads to high coronal proton temperatures and large asymptotic flow speeds when the protons are heated over a characteristic length scale of one solar radius or more. Heating of the electron gas may result in "smearing" of the heat input due to the more efficient heat conduction in the electron gas, and more of the heat will be conducted into the subsonic region of the flow. This produces a solar wind with higher proton flux and lower asymptotic flow speed. (Heating of the transition region will have a similar effect.)

This study thus illustrates how the very small proton heat flux in the outer corona found in the eight-moment two-fluid description allows for thermally driven high-speed solar wind streams, provided most of the mechanical energy flux is deposited in the proton gas in a region where the protons are collisionless.

Acknowledgements. We thank Drs. John Kohl and Viggo Hansteen for discussions and an anonymous referee for constructive comments. This work is supported by the National Aeronautics and Space Administration under grant NAG5-3192 to the Smithsonian Astrophysical Observatory and by the Research Council of Norway (NFR) under contracts 115831/431 and 121076/420.

References

Braginskii, S. I. 1965, in M. A. Leontovich (ed.), Reviews of Plasma Physics, Vol. 1, 205-311, Consultants Bureau, New York
Chapman, S. 1954, ApJ, 120, 151
Endler, F., Hammer, R., Ulmschneider, P. 1979, A&A, 73, 190
Esser, R., Habbal, S. R. 1996, in D. Winterhalter et al. (eds.), Solar Wind Eight, Proceedings of the Eighth International Solar Wind Conference held in Dana Point, CA, USA, 25-30 June 1995, Vol. 382 of *AIP Conference Proceedings*, NASA, NSF and COSPAR, American Institute of Physics, Woodbury, New York, p. 133
Esser, R., Habbal, S. R., Coles, W. A., Hollweg, J. V. 1997, J. Geophys. Res., 102, 7063
Evje, H. O., Leer, E. 1998, A&A, 329, 735
Hammer, R. 1982, ApJ, 259, 767
Hansteen, V. H., Leer, E. 1995, J. Geophys. Res., 100(A11), 21577
Hansteen, V. H., Leer, E., Holzer, T. E. 1997, ApJ, 482, 498
Hollweg, J. V., Johnson, W. 1988, J. Geophys. Res., 93(A9), 9547
Isenberg, P. A. 1990, J. Geophys. Res., 95(A5), 6437
Kohl, J. L., Strachan, L., Gardner, L. D. 1996, ApJ, 465, L141
Kopp, R. A., Holzer, T. E. 1976, Solar Phys., 49, 43
Leer, E., Holzer, T. E. 1980, J. Geophys. Res., 85(A9), 4681
Lie-Svendsen, Ø., Hansteen, V. H., Leer, E. 1997, J. Geophys. Res., 102, 4701
McComas, D. J., Phillips, J. L., Bame, S. J., Gosling, J. T., Goldstein, B. E., Neugebauer, M. 1995, Space Sci. Rev., 72, 93
McKenzie, J. F., Banaszkiewicz, M., Axford, W. I. 1995, A&A, 303, L45
Munro, R. H., Jackson, B. V. 1977, ApJ, 213, 874
Olsen, E. L., Leer, E. 1996, J. Geophys. Res., 101, 15591
Sandbæk, Ø., Leer, E. 1995, ApJ, 454, 486
Sandbæk, Ø., Leer, E., Hansteen, V. H. 1994, ApJ, 436, 390
Schunk, R. W. 1977, Rev. Geophys. and Space Physics, 15(4), 429
Spitzer, L., Härm, R. 1953, Phys. Rev., 89, 977
Tu, C.-Y., Marsch, E. 1997, Solar Phys., 171, 363
Wang, Y.-M. 1993, ApJ, 410, L123
Withbroe, G. L. 1988, ApJ, 325, 442